Event-Shape Analysis: Sequential versus Simultaneous Multifragment Emission

D. A. Cebra, S. Howden, J. Karn, A. Nadasen,[a] C. A. Ogilvie,[b] A. Vander Molen, G. D. Westfall, W. K. Wilson, and J. S. Winfield

National Superconducting Cyclotron Laboratory and Department of Physics and Astronomy, Michigan State University, East Lansing, Michigan 48824-1321

E. Norbeck

Department of Physics, University of Iowa, Iowa City, Iowa 52242

(Received 22 September 1989; revised manuscript received 14 March 1990)

The Michigan State University 4π array has been used to select central-impact-parameter events from the reaction $^{40}Ar+^{51}V$ at incident energies from 35 to 85 MeV/nucleon. The event shape in momentum space is an observable which is shown to be sensitive to the dynamics of the fragmentation process. A comparison of the experimental event-shape distribution to sequential- and simultaneous-decay predictions suggests that a transition in the breakup process may have occurred. At 35 MeV/nucleon, a sequential-decay simulation reproduces the data. For the higher energies, the experimental distributions fall between the two contrasting predictions.

PACS numbers: 25.70.Np

It has been proposed that a multifragment reaction mechanism should become dominant at bombarding energies per nucleon above the Fermi energy.[1-4] This process should be characterized by a simultaneous dissociation of the system into many fragments. Early attempts to identify this mechanism relied only on multiplicity distributions.[5-7] It has, however, been demonstrated that information from such distributions or other inclusive observables alone is insufficient to identify conclusively multifragmentation.[8,9] Models of other processes also can account for these inclusive results. A definitive identification of this process requires study of an observable which is sensitive to the time scale of the disassembly, and not merely to the final distributions of fragments and their energies.[9,10] Studies addressing this question of the fragmentation time scale have been attempted,[11-17] however, the results remain inconclusive.

In this Letter we use an observable that has recently been proposed to be sensitive to the time scale of the fragmentation process.[9] This observable is the spheroidal shape of the envelope of the energy flow from the reaction or the event shape.[4] The emission of fragments from a simultaneous multifragmentation process will be isotropic in the center-of-mass frame and therefore the events should be spherical in shape. Conversely, sequential emission should lead to an event shape that is elongated along one axis due to the kinematical constraints of the binary decays and the time-ordered emission of the fragments. In the following analysis, we shall compare the average event shapes extracted from our experimental data to predictions from simulations of both a sequential decay and a simultaneous multifragmentation.

We have studied the system $^{40}Ar+^{51}V$ using the Michigan State University (MSU) array[18] with beams provided by the K500 and K1200 cyclotrons. Six incident energies were studied: 35, 45, 55, 65, 75, and 85 MeV/nucleon. At the time of these experiments, the 4π array consisted of 170 close-packed phoswich detectors covering an angular range from 20° to 160°. An additional 45 phoswich detectors were installed in the forward wedge to extend angular coverage from 20° to 7°. The data from the forward array were used only in the determination of the impact parameter and not in the event-shape analysis to suppress the contribution of projectilelike spectator matter. The minimum energy required for a charged particle to be detected was 4 MeV/nucleon. However, in order for a fragment to be identified it had to penetrate into the stopping scintillator, which required 20 MeV/nucleon. For identified particles, we had an isotropic resolution for $Z=1$ fragments, and charge resolution up to $Z=8$. Particles with energies from 4 to 20 MeV/nucleon were stopped in the ΔE scintillator and were assigned an estimated charge and energy for this analysis.

In the event-shape analysis technique, one first transforms the observed event into the center-of-mass frame and then conducts a kinetic-flow tensor

$$F_{ij}=\sum_n \frac{p_i^{(n)}p_j^{(n)}}{2m_n},$$

where $p_i^{(n)}$ denotes a momentum component of the nth particle and m_n denotes its mass. One uses the ordered eigenvalues of this tensor, $t_1<t_2<t_3$, to define three reduced quantities[19]

$$q_i=t_i^2\Big/\sum_{j=1}^{3} t_j^2$$

from which one determines the sphericity $S=\frac{3}{2}(1-q_3)$ and the coplanarity $C=\frac{1}{2}\sqrt{3}(q_2-q_1)$ as defined by Fai

and Randrup[4] and applied to this problem by López and Randrup.[9] The eigenvectors of the kinetic-flow tensor represent the axes that best approximate the envelope of the outgoing energy-flow vectors of the fragments. The sphericity parameter represents the relative strength of the third (major) axis with respect to the other two axes, and is a measure of the amount of elongation. A spherical distribution would have three equal axes ($q_1=q_2=q_3=\frac{1}{3}$), which results in a sphericity equal to 1.0. The coplanarity parameter represents the asymmetry between the two minor axes. A spherical distribution would have a coplanarity of 0.0, while a flattened distribution will have an extremely small q_1 axis, and, therefore, the coplanarity parameter will be large. The data presented in this Letter are in the form of sphericity versus coplanarity distributions or centroids, and conclusions will be based upon comparisons between experimental data and predictions from simulations.

We performed simulations of both sequential and simultaneous breakup processes. These sequential simulations assumed a stationary system with excitation energy from 8 to 20 MeV/nucleon which cooled through emission of energetic fragments. The mass and charge of the emitted fragments were chosen from a distribution of possible exit channels. The probability for each breakup channel was taken to be $\exp(-\Delta E/\tau)$, where ΔE is the energy difference between the initial and final states and τ is the temperature of the excited system. The temperature at each stage in the decay was determined assuming $E^*=a\tau^2$, where a is the level-density parameter. After a channel had been selected, a breakup energy was assigned based on the Boltzmann distribution and a Coulomb energy was calculated assuming an emission distance of $1.22(A_1^{1/3}+A_2^{1/3})$ fm. Each of the daughters received a share weighted by mass (equal temperature) of the remaining excitation energy. The daughters continued to decay until fragment emission was no longer energetically possible. Events for the simultaneous simulation were generated by randomizing the emission directions of the outgoing fragments produced from the sequential simulation. This ensured that the first-order predictions of the two models were identical. These simulated events were filtered through a software replica of our detector[20] and analyzed in the same manner as our experimental data.

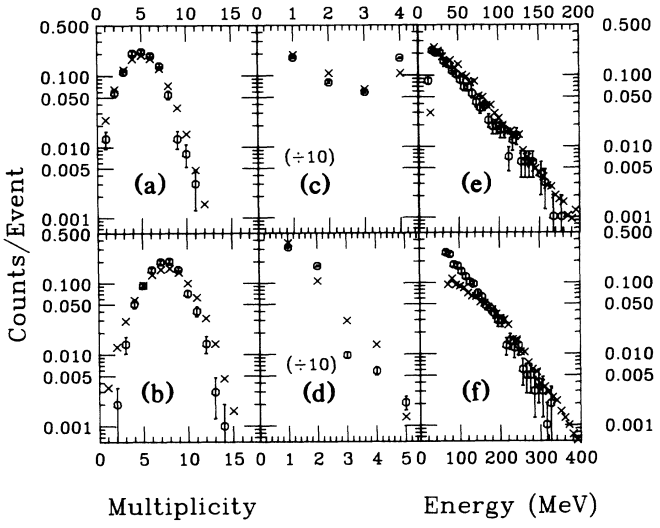

FIG. 1. A comparison of the results from simulations (open circles) to the experimental (crosses) data for the 65-MeV/nucleon case. Six observables are compared: (a) the multiplicity of identified charged particles, (b) total detected charged-particle multiplicity (includes particles that stop in the ΔE scintillator), (c) mass distributions for light particles, (d) charge distributions, (e) kinetic-energy distributions for protons, and (f) kinetic-energy distributions for helium ions.

We first demonstrate that the inclusive observables are correctly given by the simulation. Discrepancies in these observables will cause differences in the multiparticle observables that are unrelated to the effect of interest. Figure 1 displays these observables for the 65-MeV/nucleon case. The quantities that are compared include both the total detected charged-particle multiplicity and the multiplicity of identified particles, the mass and charge distributions, and the kinetic-energy spectra for protons and helium ions. It is clear from Fig. 1 that the simulation accurately reproduces the basic observables of the experimental data. Similar reproductions of these observables have been obtained at the other energies studied.

Contour plots of the predicted shape distributions for the simulated sequential breakup process and the simultaneous multifragmentation are shown in Fig. 2 for the 65-MeV/nucleon case. The shape distribution for the sequential events [Fig. 2(a)] is that of a flattened prolate spheroid (a long primary axis and an extremely short tertiary axis). This interpretation of the shape distribution is made by observing the steepness of the contours with respect to the line from (0,0) to (0.75,0.43), which corresponds to two-dimensional shapes. The elongation of the primary axis suggests a strong kinematic constraint caused by the initial decays of the system. These earliest decays occur when the system is maximally heated; thus, these decays carry off the most energy and there is a large relative momentum between the two daughters. The later decays occur after the system has cooled and are less likely to define the principal axes.

A simultaneous process does not contain the cooling through particle emission or the emission-by-emission momentum conservation that would lead to elongation in one or two principal axes. It should produce spherical event shapes in the limit of infinite multiplicity. The event-shape distribution displayed in Fig. 2(c) is on average less prolate (a larger sphericity) than the previous simulation. The sphericity and coplanarity centroids of these two simulations are displayed in Fig. 3 for all the bombarding energies studied. The clear separation of these centroids confirms that this technique provides an observable capable of resolving between sequential and

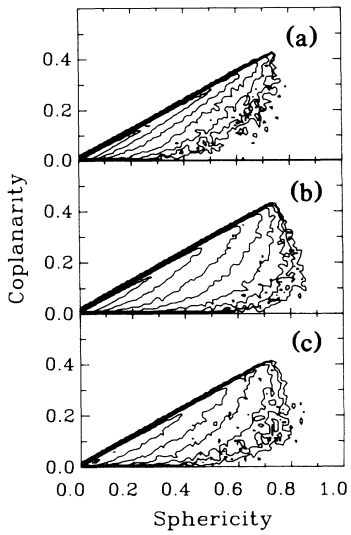

FIG. 2. A comparison of the distribution of event shapes for the 65-MeV/nucleon $^{40}Ar+^{51}V$ case from (a) a simulation of a sequential binary decay process, (b) the experimental data, and (c) a simulation of a simultaneous multifragmentation. Both simulations have been filtered through the acceptance of the MSU 4π array. Three contours correspond to 1 order of magnitude.

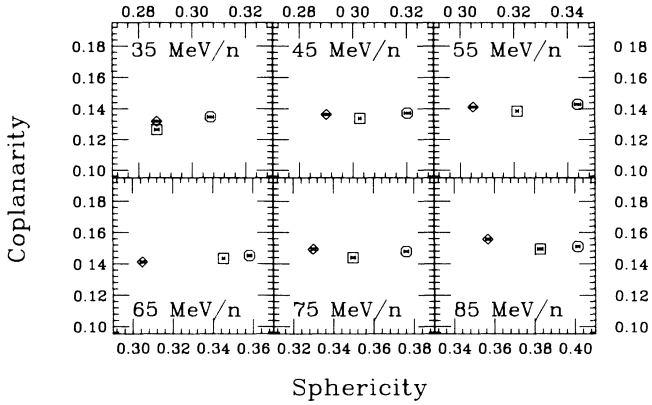

FIG. 3. A study of the average sphericity and coplanarity values as a function of beam energy for the system $^{40}Ar+^{51}V$. The centroids of the sequential simulation are represented by diamonds, those of the experimental data are represented by squares, and those of the simultaneous simulation are represented by circles. The uncertainties displayed are statistical errors of the mean. An estimate of potential systematic errors is given in the text.

simultaneous multifragmentation.

Physical processes other than sequential emission may also produce an elongation in the event shape. Examples of such processes include rotation of the interaction region, collective flow, finite multiplicity, and spectator matter. We have performed simple simulations for these processes for the 35-MeV/nucleon case (where these effects are expected to be the most severe). For the quantities of flow measured in these data,[21] we expect the induced elongation to be -0.005 unit of sphericity and $+0.003$ unit of coplanarity. Rotational effects are expected to induce a maximum of -0.01 unit of sphericity and $+0.001$ unit of coplanarity. These two effects induce elongations that are only one-eighth the size of the observed difference between the two simulations. The finite multiplicity produces the majority of the observed elongation in both of the simulations. However, by generating the simultaneous events from sequential events, one constrains the multiplicity, and this ensures that any observed differences must come from kinematical effects. Elongations induced by spectator matter have been minimized by excluding the information from the forward wedge.

The shape distribution for the 65-MeV/nucleon experimental data is shown in Fig. 2(b). The events used for this analysis have been gated on impact parameter and only the most central ($\bar{b} \approx 0.3 b_{max}$, where $b_{max} = R_{Ar} + R_V$) collisions have been selected. The determination of the centrality was made on an event-by-event basis using the total detected charge of fragments in the midrapidity range ($0.75 y_{targ} < y_{frag} < 0.75 y_{proj}$).[20] Figure 3 displays the sphericity and coplanarity centroids as a function of beam energy for the experimental data and for the two simulations. For the 35-MeV/nucleon case, the centroids are almost identical to those predicted for sequential decay. For energies greater than 35 MeV/nucleon, the experimental centroids fall between the two predicted values indicating that the pure sequential model does not apply for these energies. Clearly from 35 to 65 MeV/nucleon, there is a progression from the sequential extreme towards the simultaneous extreme. It was not feasible to study bombarding energies below 35 MeV/nucleon due to the low-energy thresholds; therefore, we present only a single energy which is suggestive of sequential decay. However, the conclusion that sequential decay dominates at and below this energy is consistent with previous results. The experimental centroids do not reach the values predicted for the simultaneous simulation. This may be due to the effects of other physical processes not considered. Additionally, for the purposes of this analysis, simultaneous multifragmentation has been defined as completely isotropic emission, which may be an unrealistic requirement.

We conclude from this analysis that the kinematical constraints and the time-ordered emission implicit in a sequential-decay process create an observable elongation in the predicted event shape. There is a clear separation between the centroids of the event-shape distributions predicted for a sequential decay and a simultaneous multifragmentation, indicating that this multiparticle observable is sensitive to the breakup dynamics. At 35 MeV/nucleon, the event-shape distribution determined from our experimental data agrees with that predicted for the simple sequential decay. At this energy, the

center-of-mass velocity is well below the Fermi velocity and mean-field effects are strong. Thus, sequential decay is expected to play an important role in the deexcitation process. At higher bombarding energies, the experimental distributions fall between the simulations for sequential and simultaneous decay. This suggests the onset of simultaneous multifragmentation processes and an increase in their relative importance as the beam energy increases.

This work was supported by the National Science Foundation under Grant No. PHY-86-11210. The collaboration with E. Norbeck was supported by the Research Corporation. The authors would like to acknowledge T. Li for his work on the rotational simulations.

[a]Permanent address: University of Michigan, 4901 Evergreen Road, Dearborn, MI 48128.

[b]Current address: Gesellschaft fur Schwerionenforschung, D-6100 Darmstadt, West Germany.

[1]J. P. Bondorf *et al.*, Phys. Lett. **150B**, 57 (1985).

[2]D. H. E. Gross *et al.*, Phys. Rev. Lett. **56**, 1544 (1986).

[3]J. Randrup and S. E. Koonin, Nucl. Phys. **A356**, 223 (1981).

[4]G. Fai and J. Randrup, Nucl. Phys. **A404**, 551 (1983).

[5]K. R. G. Doss *et al.*, Phys. Rev. Lett. **59**, 2720 (1987).

[6]G. Klotz-Engmann *et al.*, Phys. Lett. B **187**, 245 (1987).

[7]J. W. Harris *et al.*, Nucl. Phys. **A471**, 241c (1987).

[8]L. G. Moretto and G. J. Wozniak, Nucl. Phys. **A488**, 337c (1988).

[9]J. A. López and J. Randrup, Nucl. Phys. **A491**, 477 (1989).

[10]B. V. Jacak, Nucl. Phys. **A488**, 325c (1988).

[11]R. Bougault *et al.*, Nucl. Phys. **A488**, 255c (1988).

[12]R. Trockel *et al.*, Phys. Rev. Lett. **59**, 2844 (1987).

[13]Y. Cassagnou *et al.*, in *Nuclear Dynamics and Nuclear Disassembly,* edited by J. B. Natowitz (World Scientific, Singapore, 1989), p. 386.

[14]J. Pochodzalla, Nucl. Phys. **A488**, 353c (1988).

[15]J. Pouliot *et al.*, in *Nuclear Dynamics and Nuclear Disassembly* (Ref. 13), p. 42.

[16]J. Pouliot *et al.*, Phys. Lett. B **223**, 16 (1989).

[17]B. A. Harmon *et al.*, Nucl. Instrum. Methods Phys. Res., Sect. A **238**, 347 (1985).

[19]M. Gyulassy, K. A. Frankel, and H. Stöcker, Phys. Lett. **110B**, 185 (1982).

[20]C. A. Ogilvie *et al.*, Phys. Rev. C **40**, 654 (1989).

[21]C. A. Ogilvie *et al.*, Phys. Rev. C **40**, 2592 (1989).